HOW PORE MOUTH CHARGE DISTRIBUTIONS ALTER THE PERMEABILITY OF TRANSMEMBRANE IONIC CHANNELS

PETER C. JORDAN
Department of Chemistry, Brandeis University, Waltham, Massachusetts 02254

ABSTRACT This paper investigates the effects that surface dipole layers and surface charge layers along the pore mouth–water interface can have on the electrical properties of a transmembrane channel. Three specific molecular sources are considered: dipole layers formed by membrane phospholipids, dipole layers lining the mouth of a channel-forming protein, and charged groups in the mouth of a channel-forming protein. We find, consistent with previous work, that changing the lipid–water potential difference only influences channel conduction if the rate-limiting step takes place well inside the channel constriction. We find that either mouth dipoles or mouth charges can act as powerful ion attractors increasing either cation or anion concentration near the channel entrance to many times its bulk value, especially at low ionic strengths. The effects are sufficient to reconcile the apparently contradictory properties of high selectivity and high conductivity, observed for a number of K^+ channel systems. We find that localizing the electrical sources closer to the constriction entrance substantially increases their effectiveness as ion attractors; this phenomenon is especially marked for dipolar distributions. An approximate treatment of electrolyte shielding is used to discriminate between the various mechanisms for increasing ionic concentration near the constriction entrance. Dipolar potentials are far less sensitive to ionic strength variation than potentials due to fixed charges. We suggest that the K^+ channel from sarcoplasmic reticulum does not have a fixed negative charge near the constriction entrance; we suggest further that the Ca^{+2}-activated K^+ channel from transverse tubule does have such a charge.

INTRODUCTION

It is generally recognized that long range electrostatic interactions have a major influence on ionic transport across lipid membranes (Parsegian, 1969; Levitt, 1978; Jordan, 1982, 1983, 1986). These forces act in two distinct domains: the membrane itself and the aqueous regions surrounding it. If ion transport is mediated by channel-forming proteins, the transmembrane region is the channel constriction. In a narrow pore the long range electrostatics only modulate the direct interaction of an ion with various charged and polar groups; the dominant forces are the local interactions that control channel selectivity. This is the domain of translocation — the process of traversing the channel — and of dehydration/hydration — the process of entering (or exiting) the channel. The other region is the aqueous medium bathing the membrane and occupying the mouths of the channel. Here, long range electrostatic forces have a major influence on ionic motion; they cause both polarization (image forces) and electrolyte shielding. This is the domain of diffusion up to and away from the channel.

Electrostatic calculations that focus upon the channel interior are subject to a number of serious limitations. The pore is treated as a uniform cylinder. The water within the pore is presumed to be dielectrically equivalent to bulk water, even though it is known to have quite a different structure (Mackay et al., 1984; Lee and Jordan, 1984). As a result, such calculations can only provide a qualitative indication of the effect that varying structural and electrical features of the water–ion–pore former–membrane ensemble can have on the energy profile for ions within the constriction.

The situation is rather different when the focus is on the electrical properties of the channel mouth. Structural data on the acetylcholine receptor channel (Kistler and Stroud, 1981), electrodiffusion models of the delayed rectifier K^+ channel (Armstrong, 1975), and kinetic models of high conductance K^+ channels (Miller, 1982*a*) all share a common feature. The entrance to the channel constriction is a fairly large mouth region in which many water molecules can reside; the aqueous structure in this domain should be similar to that of bulk water. Thus, calculations describing the effect that changes in the electrical and structural properties of the channel former have on the energy profile for an ion in the channel mouth should be rather more reliable quantitatively.

This paper studies the influence that three particular charge distributions may have on ion permeation. First we reinvestigate the effect that the membrane dipole potential (the lipid–water potential difference) has on the energy profile within the channel constriction (Jordan, 1983,

1984*a*). Fairly realistic pore geometries are treated. There is a constant diameter constriction attached to mouths that flare outward, as illustrated in Fig. 1. Two distinct cases are considered: (*a*) The channel-forming protein protrudes through the bilayer so that the phospholipid membrane (and thus the origin of the membrane dipole potential) terminates a considerable distance from the channel axis. (*b*) The channel-forming protein is encapsulated by the bilayer; the phospholipid molecules themselves form the pore mouth. This source terminates close to the channel axis. The results are used to interpret recent data on the effect that variation of the lipid–water potential difference has on the conductance of gramicidin-A and its analogues.

The other calculations, of which a preliminary account has already appeared (Jordan, 1985), focus on properties of the pore mouth and study how surface charges and surface dipoles at the pore mouth–water interface can affect ionic concentration at the entrance to the constriction. The question of special interest is how large can the local mouth potentials be for realistic charge or dipole distributions. The impetus for this study is the existence of a number of highly permeable, yet highly selective, K^+ channels (Coronado et al., 1980; Latorre et al., 1982; Moczydlowski et al., 1985). Only if the ionic concentration near the constriction entrance is many times its bulk value can the contradictory properties of high permeability and high selectivity be reconciled. The calculations demonstrate this to be feasible.

Finally, because the potential due to fixed charge distributions are likely to be highly dependent upon ionic strength, we present a heuristic method to account for electrolyte shielding. We find that dipolar potentials are far less sensitive to ionic strength variation than potentials due to an ionic source. This provides evidence for discriminating among the various possible ways in which cation concentration near the channel entrance can be larger than bulk concentration. Our analysis suggests that in the K^+ channel from sarcoplasmic reticulum (SR) there cannot be a fixed negative charge near the channel entrance. It also indicates that for the Ca^{+2}-activated K^+ channel from transverse tubule (TT) there must be such a fixed negative charge.

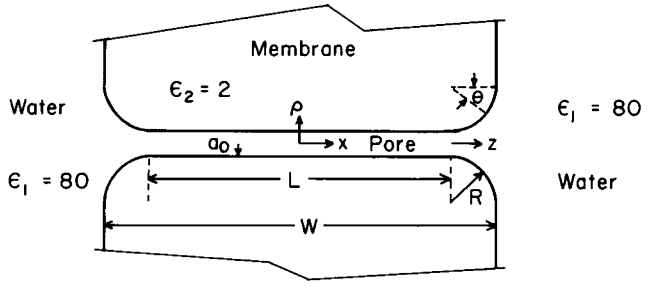

FIGURE 1 Cross-section of a cylindrical pore spanning a membrane of dielectric constant, ϵ_2. The pore interior and the water are presumed to have the same dielectric constant ϵ_1. The membrane width is W, the constriction length is L, the radius of the mouth opening is R, and the constriction radius is a_0. The structural parameters describing the model are $\delta = W/2a_0$, $\beta = L/2a_0$, and $b = R/a_0$. The distance x is measured from the center of the pore; z is measured from the entrance to the constriction. Surface charge distributions are located on the curved mouth surfaces; dipolar distributions are located along the mouths or at the water–membrane surface.

THEORY

The model geometry for the systems considered is illustrated in Fig. 1. Cylindrically symmetrical electrical sources are located at the membrane–water interface or at the pore mouth–water interface. The electrical potential at any point in the system can then be calculated using the replacement charge density approach (Levitt, 1978; Jordan, 1982). The optimal method is determined by the dielectric geometry of the system; the approach required for treating pore structures like those of Fig. 1 was the subject of an earlier study (Jordan, 1984*a*). In this paper we investigate the consequences of three different electrical sources: the membrane dipole potential (the lipid–water potential difference), dipolar charge distributions located along the pore mouth, and surface charge distributions located along the pore mouth. The mathematical description of the first of these sources has been given previously (Jordan, 1983). That needed for consideration of the other two is presented here.

Consider a cylindrically symmetric surface charge density $\sigma_0 f(\theta)$ on the right-hand mouth of the model pore; the angular dependence permits consideration of non-uniform distribution. The bare potential due to such a charge distribution is

$$V_\sigma(r) = (\sigma_0 R/\epsilon_i) \int_0^{\pi/2} d\theta f(\theta)\rho(\theta) \int_0^{2\pi} d\phi D^{-1}, \quad (1)$$

where $D = [r^2 + \rho^2 - 2r\rho\cos\theta + (\xi - x)^2]^{1/2}$; r and x are coordinates in space, whereas ρ and ξ are coordinates of the surface on which the charges are located. Integration over ϕ yields

$$V_\sigma(r) = (4R\sigma_0/\epsilon_i) \int_0^{\pi/2} d\theta f(\theta)\rho K(k)/S \quad (2a)$$

$$S = \sqrt{(\xi - x)^2 + (\rho + r)^2}, \qquad k = 2\sqrt{\rho r/S}. \quad (2b)$$

$K(k)$ is the complete elliptic integral of the first kind (Abramowitz and Stegun, 1965); ϵ_i is either ϵ_1 or ϵ_2 depending upon whether the charge distribution is located just to the right or left of the dielectric discontinuity (in the high or low dielectric constant region). The pore potential due to this source can be calculated by the replacement charge density method (Jordan, 1982, 1984*b*), which requires as input the normal component of the electric field at electrical phase boundary, $n \cdot \nabla V_\sigma$ with n pointing outward. In this calculation we describe the electrical source as a set of fixed charges located in the high ϵ domain just to the right of the electrical phase boundary. As such, they cannot create a set of electrical images in the immedi-

ately adjacent region of the mouth. They do, however, polarize the more distant regions of the lipid and the pore former. An actual physical system does not have a cylindrically symmetric distribution of charge. The source must be a fixed charge, either close to the channel entrance or far from it. By altering the form of $f(\theta)$ we can mimic the effect of locating the charge close to or far from the entrance. This does not eliminate the feature of cylindrical symmetry. However, this approach is the first term in a Fourier expression; calculations treating non-axial ionic sources indicate that the lowest order term in such an expansion (the cylindrically symmetric term) determines the axial potential.[1]

Construction of the source potential due to surface dipoles lining the pore entrance is readily accomplished. The bare potential for a cylindrically symmetric dipole distribution, $\mu_0 f(\theta)$ is

$$V_\mu(r) = (\mu_0 R/\epsilon_i) \int_0^{\pi/2} d\theta f(\theta)\rho(\theta) \int_0^{2\pi} d\theta B/D^3, \quad (3)$$

where $B = (\xi - x)\cos\theta + (r\cos\phi - \rho)\sin\theta$ and D is the same as in Eq. 1. Integration over ϕ yields the result

$$V_\mu(r) = (4R\mu_0/\epsilon_i) \int_0^{\pi/2} d\theta [f(\theta)/S] \cdot [\sin\theta(E - K)/2 - \rho HE/T^2] \quad (4a)$$

$$T^2 = S^2 - 4\rho R, \quad H = (\xi - x)\cos\theta + (r - \rho)\sin\theta. \quad (4b)$$

Here, S, k, and K are the same as in Eq. 1; E is the complete elliptic integral of the second kind (Abramowitz and Stegun, 1965). Using the source potential $V_\mu(r)$, the electric field at the dielectric interface, $n \cdot \nabla V_\mu(r)$, can be calculated and the formalism of the replacement charge density method used to compute the pore potential.

Exact solution of the electrostatic equations requires matching boundary conditions at all points on an infinite dielectric interface; thus, numerical calculations are necessarily approximate. The infinite water–membrane interface must be cut off at a maximum value of ρ and the boundary conditions can only be satisfied at a finite number of points (Jordan, 1982, 1983). To obtain accuracy of better than 0.5%, many points were required: 42 along the water–membrane interface, up to 36 along the arc, and up to 62 along the pore interior. A ρ_{max} of 37.5 (in units of a_0) was used.

RESULTS AND DISCUSSION

Overview

In this section we consider both the general consequences of our calculations and some specific applications to questions of biophysical significance. We first extend our previous treatment of the membrane dipole potential (Jordan, 1983), describing its general features and some possible physiological consequences and then making specific application to gramicidin. We then describe the general behavior of the electric potential created by a variety of possible dipole and charge distributions along the pore mouth–water interface and indicate how such electrical sources could be responsible for anomalous properties of the K^+ channel from SR and of the Ca^{+2}-activated K^+ channel from TT. Finally, we incorporate a discussion of electrolyte shielding to demonstrate that our approach permits a quantitative description of the conductance–concentration data on these two systems.

Membrane Dipole Potential : General Features

Symmetrical pores with the gross dielectric structure illustrated in Fig. 1 can be formed in two general ways. These differ depending upon how the pore former is incorporated into the membrane. The extreme cases are contrasted in Figs. 2 and 3. In the first instance, the pore former projects through the membrane, and the lipid bilayer terminates a substantial distance from the axis of the pore. The mouth of the pore is a structural feature of the pore former. In the second limiting case, the pore former is encapsulated by the membrane. The pore mouth is formed by the phospholipid molecules of the bilayer. In these figures, the values of β and δ selected describe a wide range of realizable pore structures: membrane widths between 3 and 6 nm, constriction lengths between 1 and 2 nm, and constriction radii between 0.15 and 0.25 nm.

In case 1 the polar head groups of the phospholipid are not part of any electrical source along the pore mouth–water interface because the membrane terminates outside the mouth region. In case 2 the polar head groups form the source of whatever charge distribution is present along that interface. The size of the interfacial potential step, which may vary with position on the interface, depends upon the orientation and packing of the head groups. Since this electrical source is a function of membrane composition, it contributes to the shielded membrane dipole potential in the pore.

The quantity of interest is the ratio of the shielded membrane dipole potential in the pore interior, V, to the water–membrane potential difference, V_0. This function, F, depends not only on the mode of pore former incorporation and on the phospholipid orientation at the pore mouth–water interface, but also on the reduced membrane width, $\delta \equiv W/2a_0$, reduced constriction length, $\beta \equiv L/2a_0$, and reduced distance from the pore center, $\xi = x/a_0$, as well as the dielectric ratio, $K \equiv \epsilon_1/\epsilon_2$ that describes the electrical dissimilarity of the two phases,

$$V = V_0 F(\xi; \beta; \delta; K). \quad (5)$$

The ratio V/V_0 is also, in principle, a function of the radial as well as the axial coordinate. However, in a continuum approximation where the pore interior is a homogeneous

[1]Vayl, I. S., and P. C. Jordan, unpublished results.

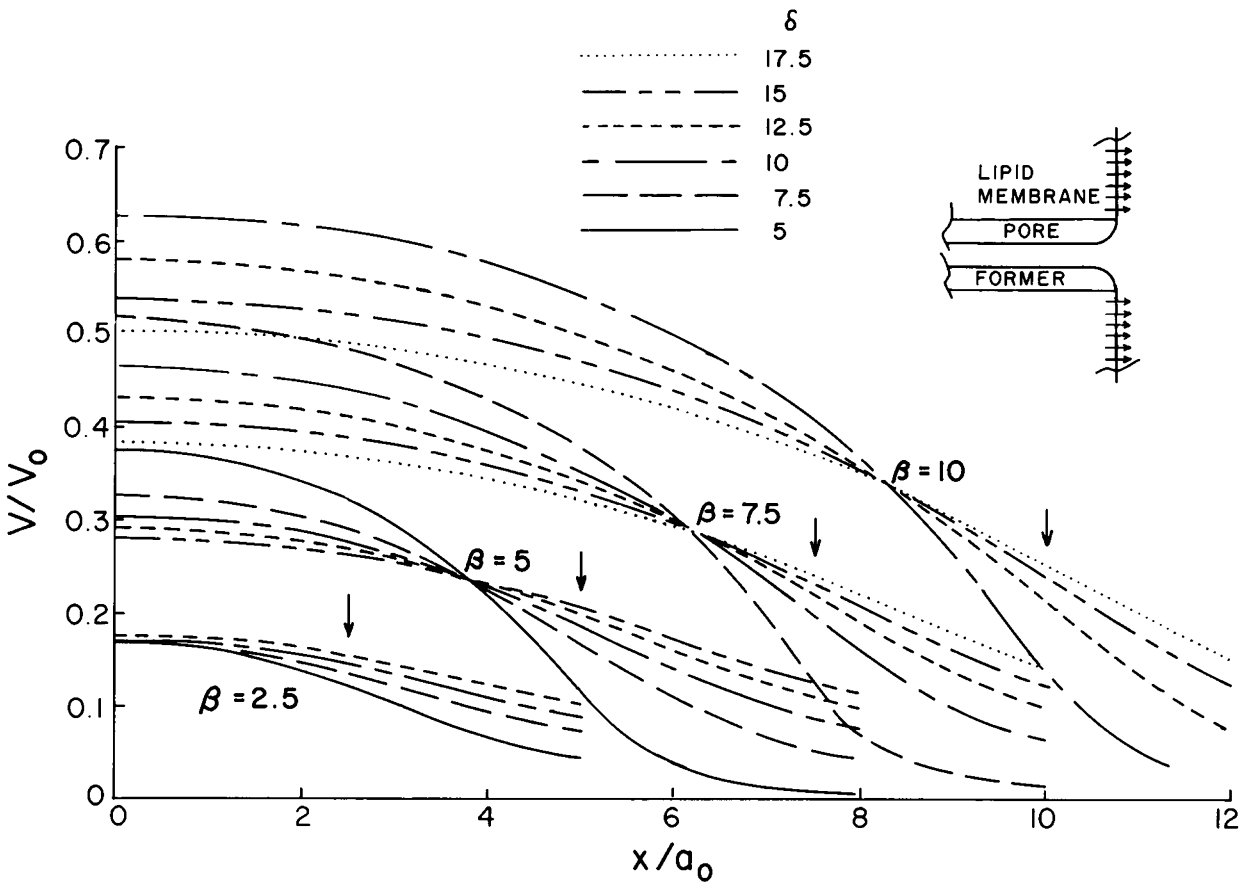

FIGURE 2 Axial potential due to the membrane dipole potential (lipid–water potential difference). The source is modeled by point dipoles at the electrical phase boundary with bulk water. The reduced distance, X/a_0, is measured from the midpoint of the membrane. The effects of variation of reduced membrane width, $\delta = W/2a_0$, and reduced constriction length, $\beta = L/2a_0$, are illustrated. The values selected describe a wide range of potentially realizable pore structures. The dielectric ratio is 40. Here, the pore former protrudes through the membrane, and the source stops at the pore former–membrane junction. The vertical arrows indicate the location of the constriction entrance.

dielectric, the radial dependence is totally insignificant for a dielectric ratio of 40, representative of lipid water systems. In any plane perpendicular to the pore axis the variation in F is $<1\%$ for $0 \leq r \leq 0.6a_0$, an observation consistent with Levitt's conclusions with respect to potential variation in cylindrical pores for axial, ionic sources (Levitt, 1985).

The model geometries being studied are somewhat artificial. Altering the pore mouth radius, R, alters the proximity of the phospholipids of the membrane to the aqueous pore. In this study the thickness of the channel protein and the size of the channel vestibule are not independently variable. Nonetheless, some general conclusions, which are entirely compatible with earlier observations (Jordan, 1983, 1986), can be drawn about the effect of structural variation on the shielding of the membrane dipole potential. The electrical source illustrated in Fig. 2 can arise in one of two ways. As already indicated, the pore former may project through the membrane. Alternatively, the pore mouth could still be formed by phospholipids, but the structural reorganization required in this region could so severely disrupt head group packing that there would be little or no potential step in passing through the interface.

The computations for the model of Fig. 2 can be tested by comparing results for the geometry of Fig. 1 with those for which the pore has sharp corners, i.e., when $b = 0$ (Jordan, 1983). If L is increased until it equals W, the inequality

$$F(\xi; \beta; \delta; K) - F(\xi; \delta; \delta, K) < 0 \qquad (6)$$

must be obeyed. Values of $b = \delta - \beta$ as small as 0.5 were tested and the difference (Eq. 6) decreased uniformly as $b \rightarrow 0$. Shrinking W until it equals L provides no similar test since the process alters the system in competing ways; the source is brought closer to the axis, tending to increase F, and the membrane is narrowed, tending to decrease F. Most commonly, the inequality is

$$F(\xi; \beta; \delta; K) - F(\xi; \beta; \beta; K) > 0, \qquad (7)$$

a result that is always true if $\xi > \beta$. In the interior of the pore, as long as b is not too large, the inequality is reversed.

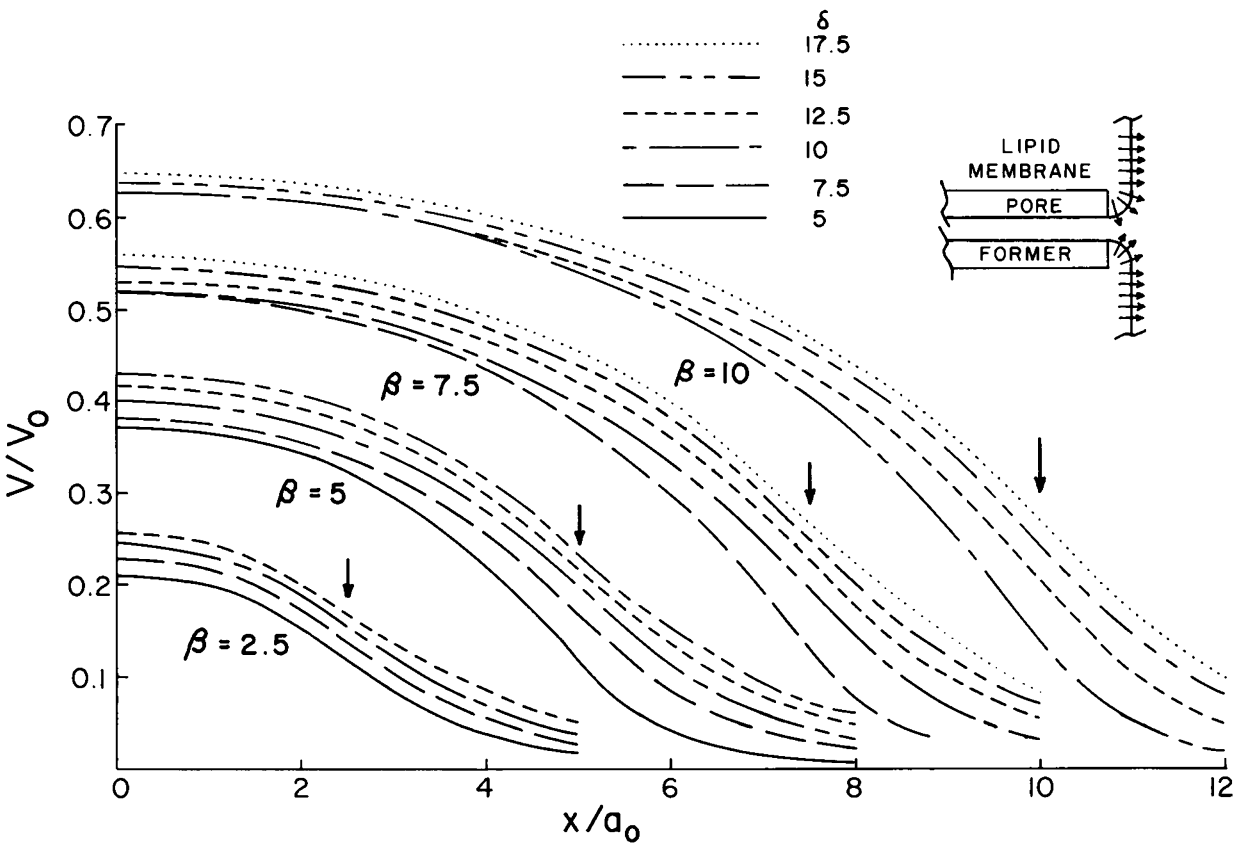

FIGURE 3 Axial potential due to the membrane dipole potential. Conventions are the same as in Fig. 2. The pore former is encapsulated by the lipid bilayer. The phospholipid molecules form the mouth region.

If the pore former is encapsulated, as illustrated in Fig. 3, the qualitative picture differs substantially in the interior of the constriction. Increasing the membrane width increases the dipole potential. The inequalities of Eqs. 6 and 7 must now always be applicable. These constraints were tested, again for b values as small as 0.5, and the differences decreased uniformly as $b \rightarrow 0$. The results that are plotted in Fig. 3 correspond to an extreme situation, no structural disruption of head group orientation forming the pore mouth. The case of gradually increasing disruption can be studied by assuming that $f(\theta) = \cos\theta$ in Eqs. 3 and 4. The qualitative picture is unaffected; however, the increase of V/V_0 with increasing membrane width is somewhat less marked.

Possible Physiological Consequences

The most significant information in Fig. 2 is the effect that pore structure has on shielding the membrane dipole potential and thereby influencing permeation kinetics. There are substantial differences depending upon the length of the constriction ($L = 2a_0\beta$) the thickness of the channel protein [$R = a_0(\delta - \beta)$]. If the rate-limiting step is dehydration near the entrance to the constriction in the channel, the peak in the reaction profile is in the vicinity of the points indicated by the vertical arrows. Even for long narrow pores ($\beta = 10$), an ion senses $\lesssim$25% of the full membrane dipole potential upon dehydration. The consequences, for channel reconstitution in such dissimilar uncharged membranes as phosphatidylcholine (PC) and glyceryl monooleate (GMO), are quite insignificant even though the difference in the membrane dipole potential is ~120 mV (Pickar and Benz, 1978). Regardless of pore former thickness or channel length, changing from PC to GMO should hardly affect cation conductance; increases of two- to threefold are the most that can be expected. If translocation is rate-limiting, much more dramatic effects are expected, especially if the constriction is long and narrow and the channel protein is not too thick. For $\beta = 7.5$, a value that is not unreasonable for the K^+ channel from squid axon (Jordan, 1986), the ion senses from 40 to 50% of the bare potential. Cation conductance in GMO should be from 7 to 11 times as large as in PC. Even for $\beta = 5$, factors of four to seven are expected.

The acetylcholine receptor (AChR) channel is known to project through the membrane (Kistler and Stroud, 1981). Here β and δ may be estimated; reasonable values are $3 < \beta < 6$ and $\delta \sim 15$ (Jordan, 1986). Open state conductance in GMO and PC should differ only slightly. Even if an interior barrier were rate-limiting, the relative conduc-

tance would certainly be <4 and possibly no <1.5. If the rate-limiting process occurs near the constriction entrance, lipid variation would have even less influence.

The basic qualitative conclusions are those that have been presented previously (Jordan, 1986). Near the constriction entrance, the shielded potential is typically only 10–25% of the lipid–water potential difference. The electrical potential is then 10–30 mV less positive when a channel is reconstituted in GMO instead of PC. Thus, if the rate-limiting step in ion permeation occurs near the channel entrance, lipid variation has little effect on conductance. In the center of a channel, shielding is much less effective. Depending upon the detailed pore geometry, the pore potential is as much as 65% of the full lipid–water potential difference. The electrical potential near the channel center may be 80 mV less positive for a system reconstituted in GMO instead of PC. For systems in which passage over an interior barrier is rate-limiting, lipid variation may significantly alter conductance; the effect is particularly noticeable if the channel protein is encapsulated by the membrane.

Gramicidin : The Test Case

The system which most closely corresponds to the model of Fig. 3 and provides a test of the theory is the gramicidin dimer. The isomer crystallized from organic solvents is ~2.6 nm long (Koeppe et al., 1978); however, this is quite possibly not the head-to-head transmembrane channel (Wallace, 1986). Structural models of the head-to-head dimer suggest it may be as long as ~2.8 nm (Urry et al., 1984). The channel is normally incorporated into membranes of substantially greater thickness. To apply the theory, it must be noted that gramicidin, like the analogous polypeptide $(\text{-Gly-Ala-})_n$ which is also formed of nonpolar residues, is probably significantly more polarizable than the lipid membrane (Tredgold and Hole, 1975). To accommodate this in the context of a two dielectric theory, the channel's electrical radius must be somewhat larger than its physical radius. Different assumptions provide different estimates of the electrical radius; the values lie between 0.24–0.026 nm (Jordan, 1983) and 0.3 nm (Levitt, 1978).

The effects of lipid variation can be understood in terms of the results presented in Fig. 3. Gramicidin-B probably has its rate-limiting step near the entrance to the pore (Andersen, 1983). Even though the membrane dipole potential is ~120 mV lower in GMO than in PC (Pickar and Benz, 1978), gramicidin's conductance in GMO is only a bit more than twice its value in PC (Bamberg et al., 1976) for membranes formed from *n*-decane that are 4.5–5.0-nm wide (Benz et al., 1975). The calculated value of the GMO–PC conductance ratio depends upon the precise location of the peak in the dehydration barrier, the value chosen for the channel length, and the estimated electrical radius. If there is no disruption of head group packing at the pore mouth, the conductance ratio is between 2.5 and 3.5. For partial disruption, the calculated conductance ratio is between 2.2 and 3.1. Neither range is inconsistent with the data; the physically more attractive assumption of partial disruption is in closer agreement.

Further corroboration of the theory is given by the gramicidin M^- system, an analogue in which the central barrier is rate-limiting (Heitz et al., 1982, 1984). When phloretin (Andersen et al., 1976; Andersen, 1978) is used to lower the potential of the lipid phase by ~100 mV, the gramicidin-M^- conductance increases five- to sixfold.[2] For membranes ~5.0 nm wide, the model presented here would suggest conductance increases of 4.7–5.4-fold (for an electrical radius of 0.25 nm) or 3.8–4.2-fold (for an electrical radius of 0.3 nm). The quoted ranges depend on how head group structure in the pore mouth differs from that along the planar water-membrane interface; the larger values are for the case of partial disruption.

Pore Mouth Charge Distributions : General Features

The calculational approach outlined has more general utility. It can be modified to show how surface dipoles and surface charges distributed along the mouth of a pore can increase the pore's apparent capture radius. As mentioned in the introduction, this is of interest because systems such as the Ca^{+2}-activated K^+ channels from TT (Latorre et al., 1982; Vergara et al., 1984) and the K^+ channel from SR (Coronado et al., 1980) exhibit the rather contradictory properties of high selectivity (indicative of a narrow pore) and high permeability (indicative of a wide pore). How can these conflicting observations be reconciled? Self evidently, this can be accomplished if the pore mouth is a region of negative potential, a situation that may arise if negatively charged amino acid residues such as glutamate or aspartate reside in the pore mouth or if the pore mouth is formed by dipolar groups with their negative ends facing the aqueous region. The issue is whether realistic charge and/or dipole distributions can accommodate the known properties of these channels and whether there is any convenient way to discriminate between these hypotheses.

Surface Dipoles

First consider dipolar distributions along a pore mouth. Figs. 4 and 5 illustrate the pore mouth potential for a range of mouth size ratios, b, as a function of distance from the entrance to the constriction, measured in units of pore mouth radius, $\zeta = z/R$. Two different distributions are contrasted. In Fig. 4, the dipole density is uniform, $f(\theta) = 1$; in Fig. 5, it is concentrated close to the channel entrance $f(\theta) = 1 - \cos\theta$. The dependence of the shielded pore mouth potential on constriction length is totally insignificant, at least as long as $\beta \geq 2.5$. This is quite similar to the case of the image potential (Jordan, 1984*b*) where, outside

[2]Andersen, O. S., and F. Heitz, personal communication.

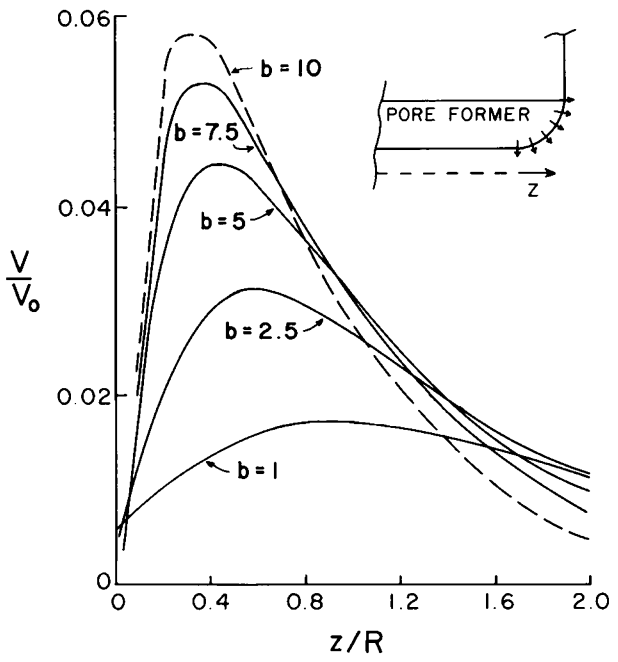

FIGURE 4 Axial potential in the aqueous region of the pore mouth due to a uniform surface dipole layer along the pore mouth–water interface. Five mouth size ratios are contrasted. The profiles are essentially independent of constriction length. The dielectric ratio is 40. Distances from the entrance to the constriction are scaled according to the size of the pore mouth.

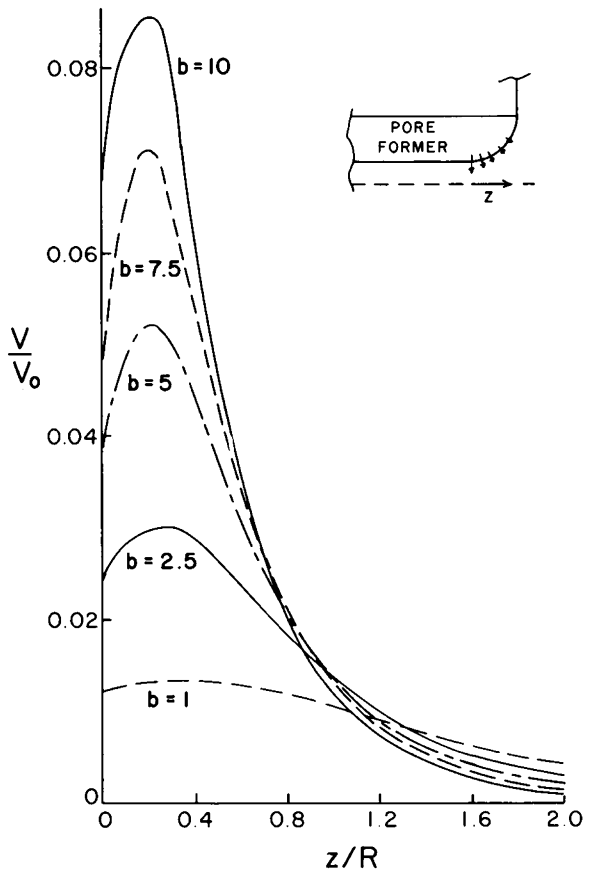

FIGURE 5 Axial potential in the aqueous region of the pore mouth due to a focussed surface dipole layer along the pore mouth–water interface. The conventions are the same as in Fig. 4.

the constriction, the electrical potentials in the channel entrance are determined only by pore mouth geometry and the dielectric dissimilarity of the phases. If anything, the phenomenon is even more marked for dipolar sources. As long as $R > a_0$, and assuming a dielectric ratio of 40, the peak in the pore mouth potential can be roughly represented as

$$V_{max} = 0.0175\, b^{0.541} V_0 \qquad f(\theta) = 1 \tag{8a}$$

$$V_{max} = 0.0137\, b^{0.809} V_0 \qquad f(\theta) = 1 - \cos\theta, \tag{8b}$$

where V_0 is the maximum potential step at the interface due to the source.

The shielded pore mouth potentials in these two cases are qualitatively similar, but quantitatively quite different. In both, the potential peaks quite close to the entrance of the constriction. In both, shielding is extensive; even for the largest value of b considered, $b = 10$, the maximum in the pore mouth potential is ~8.5% of the maximum interfacial potential step. The effect of concentrating the dipolar source near the constriction entrance is quite dramatic. The potential maximum is substantially greater, particularly for the larger pore mouths. The position of the maximum is much closer to the constriction entrance. The potential is larger in the immediate vicinity of the constriction entrance. While both the uniform and the focussed sources increase ionic concentration near the constriction entrance, it is clear that a focussed source (Fig. 5 and Eq. 8b) has a much greater effect, i.e., a focussed source makes far better use of the charge separation than a uniform one. For values of b in the range of 2.5–10, the total dipole moment along the mouth (found by integrating the dipole density on the interface) is ~20–25% as large when the distribution is focussed as when it is uniform. Even though the total source strength is smaller for the focussed source, it is more effective in increasing ionic concentration near the constriction entrance.

To provide an estimate of the vestibule potentials that might be realized, consider a dipolar array formed by peptide linkages, such as occurs in gramicidin-A (Urry, 1971). In this system the peptides form the helical backbone of the channel. Even though their orientation is far from the most favorable, they give rise to a potential step of ~450 mV in passing from the water-filled pore to the membrane interior (Jordan, 1984*a*). If one assumes the linkages are oriented to maximize the dipole moment of each peptide, each group could contribute as much as 3.7 D (1.23×10^{-29} C m) to the source of the pore mouth potential (Pethig, 1978). Using gramicidin as a guide, each peptide unit covers ~1.7×10^{-19} nm^2. The potential step at the interface due to dipolar sources is $V_0 = \mu/(\epsilon_0 \epsilon^* A)$ where μ/A is the surface dipole density, ϵ_0, the vacuum permittivity, and ϵ^*, the dielectric constant of the medium

in which the source is located. The maximum step is the ~4 V for $\epsilon^* = 2$, as would be the case if we attributed lipid-like properties to the residual surroundings of the peptide linkages. For this interfacial step, ideal dipolar alignment would permit pore mouth potentials (assuming a focussed source, see Fig. 5) in the 100–300 mV range. The estimate depends strongly on the value of ϵ^*. Dielectric measurements on nonpolar polypeptides (Tredgold and Hole, 1975) suggest that ϵ^* ~4, a value also used in analyzing protein charge distributions (Wada and Nakamura, 1981). Head group regions may be even more polarizable; local dielectric constants as large as 10 have been suggested (Flewelling and Hubbell, 1986). If ϵ^* is 4, the maximum mouth potential is between 50 and 150 mV, depending upon mouth size. If ϵ^* is 10, the largest realizable potential would be 60 mV, even if the vestibule is large. These estimates assume ideal dipole alignment; if this is not the case, the maximum realizable potentials would drop substantially.

It should be noted that studies of the peptide dipole in the α-helix (Wada, 1976; Hol, 1985) suggest that nearly ideal alignment cannot be ruled out. In this system, 97% of the dipole moment is directed axially. In addition, polarization, such as occurs in the α-helix, may increase the dipole moment per group by as much as 50% (Hol, 1985). If such a mechanism operated here, larger pore mouth potentials could be realized.

Surface Charges

Surface dipole distributions at the pore mouth–water interface can create substantial local potential differences. To determine the effect of ionizable groups, we consider three models: one with a uniform charge distribution at the interface, $f(\theta) = 1$; one with a focussed distribution, $f(\theta) = 1 - \cos\theta$; and one with a diffuse distribution, $f(\theta) = \cos\theta$. These are rather artificial simulations since such a function must be performed by one or two ionizable groups rather than by a uniformly charged surface. Nonetheless, the models provide useful insights. As indicated in the discussion of the model, treating the source as if it were cylindrically symmetric is accurate as long as consideration is limited to the axial potential. Varying $f(\theta)$ is a device to simulate moving the source closer to or farther from the constriction entrance.

Figs. 6 and 7 illustrate the pore mouth potential for a range of mouth size ratios, b, as a function of distance from the entrance to the constriction measured in units of pore mouth radius, $\zeta = z/R$. In Fig. 6, the charge density is uniform, $\sigma_0(\theta) = \sigma_0$; in Fig. 7, it is concentrated near the channel entrance, $\sigma(\theta) = \sigma_0(1 - \cos\theta)$. The pore mouth potential, V, is measured in units of $V_0 = \sigma_0 a_0/4\pi\epsilon_0\epsilon$. It is insignificantly dependent on constriction length. Just as was the case for the dipole potential, the peak in the pore mouth potential (assuming a dielectric ratio of 40) can be

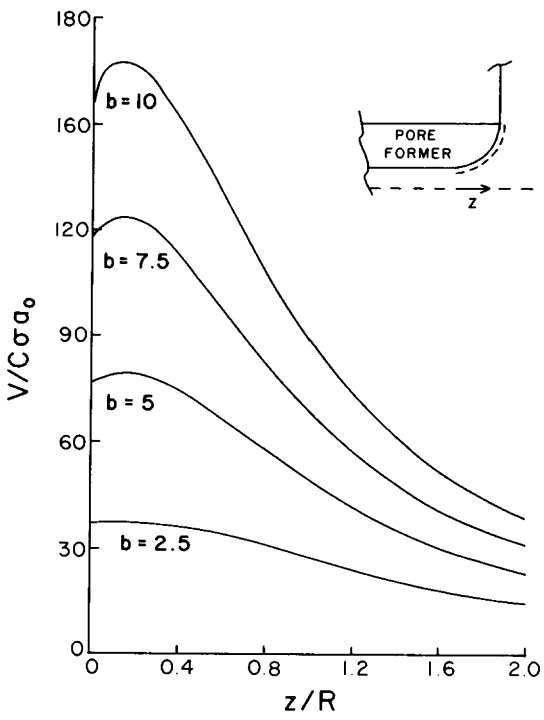

FIGURE 6 Axial potential in the aqueous region of the pore mouth due to a uniform surface charge layer along the pore mouth–water interface. The profiles are independent of constriction length. The potential is scaled in units of surface charge density, σ_0, and constriction radius, a_0. The constant C is $(4\pi\epsilon_0\epsilon_1)^{-1}$. The remaining conventions are the same as those of Fig. 4.

simply related to b

$$V = 13.56b^{1.09}V_0 \qquad \sigma(\theta) = \sigma_0 \tag{9a}$$

$$V = 5.94b^{1.15}V_0, \qquad \sigma(\theta) = \sigma_0(1 - \cos\theta). \tag{9b}$$

The nonuniform distribution clearly makes more efficient use of the total charge. For a given value of σ_0, the potential maximum is roughly half what it would be with a uniform distribution, however, the total charge is only ~20% as large. One or two ionizable groups close to the constriction entrance are as efficient in altering the electrical potential in this critical region as more than twice as much charge spread out uniformly on the surface. Locating the charges preferentially in regions distant from the constriction entrance is obviously even less effective. The same total charge, concentrated further from the mouth, $\sigma(\theta) = \sigma_0 \cos\theta$, is ~25% as effective as when it is concentrated near the mouth, $\sigma(\theta) = \sigma_0(1 - \cos\theta)$. The fact that the low dielectric constant lipid is in close proximity to the charged group is extremely important. Because the lines of force are being expelled from the lipid, there is significant amplification of the potential above the value it would have if the same charge distribution were located in bulk water. For the uniform distribution, this amplification factor is ~1.5–2 for b in the range of 2.5–10. If the charge distribution is localized there is more substantial amplifi-

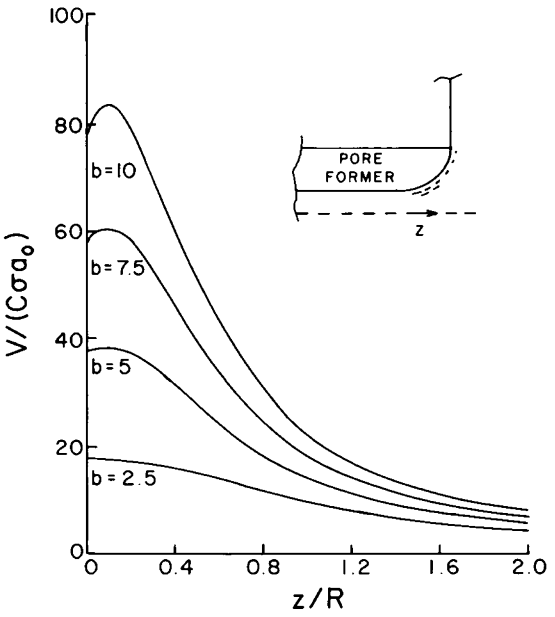

FIGURE 7 Axial potential in the aqueous region of the pore mouth due to a surface charge layer concentrated near the constriction entrance. Conventions are those of Fig. 6.

cation; it is as much as 3.5 for the largest pore mouth considered.

The potential is far more localized near the constriction entrance in the case of the concentrated source. This is also obviously advantageous since in real situations, unlike the models we are analyzing, electrolyte shielding can significantly reduce the potential. Debye shielding is less important if the potential attenuates more rapidly. Comparing Figs. 6 and 7 to Figs. 4 and 5 indicated an important way in which dipolar sources and charge sources differ; the dipole potentials are far more localized, a phenomenon especially noticeable if the source is focussed and if the pore mouth is large. This suggests that electrolyte shielding may be relatively far less important for dipolar sources.

TABLE I
PEAK PORE MOUTH POTENTIAL, AS A FUNCTION OF PORE MOUTH GEOMETRY, DUE TO A SINGLE CHARGED GROUP AT THE PORE MOUTH–WATER INTERFACE

$b \equiv R/a_0$	Focussed Source				Diffuse Source			
	Constriction entrance radius (nm)							
	0.2	0.25	0.3	0.4	0.2	0.25	0.3	0.4
	Potential (mV)							
2.5	130	104	87	65	53	42	35	27
5	118	94	79	59	36	29	24	18
7.5	105	84	70	59	27	22	18	13
10	93	75	62	47	22	17	14	11

A focussed source has the charge localized near the constriction entrance; the diffuse source has the charge located far from the constriction entrance.

How large a potential is attainable with realistic charge distributions? Table I presents the maximum in the mouth potential for various pore mouth radius ratios ($b = R/a_0$), as a function of constriction radius. The consequences of a single ionizable group, either placed near the constriction entrance or placed far from it, are contrasted (total mouth charge of one). Regardless of constriction size or pore mouth size and as long as the charged group is not too far from the entrance, a single charged group decreases the electrical potential in the mouth by >15 mV; this is sufficient to increase ionic concentrations near the constriction entrance 1.8-fold. The largest potential arises from a geometry that concentrates the charge very close to the entrance to the pore; the resultant 130 mV potential drop, if unshielded, would increase cation concentration almost 200-fold and permit small channels to exhibit enormous convergence conductance.

To obtain an idea of just how large an effect is possible under extreme conditions, Table II gives peak potentials, assuming a uniform mouth charge distribution of $2e/nm^2$, about the largest value realistically attainable (McLaughlin, 1977). The values range from 200 mV to 2.5 V, depending upon pore mouth size. Even recognizing that electrolyte shielding will substantially reduce the potential, the numbers are impressively large. A protein with such a pore mouth structure would have the ability to attract cations from anywhere in the surrounding electrolyte; it could be extremely selective and extremely permeable at the same time. Naturally, potentials as high as 1.5 V are out of the question for real systems (for a pore mouth radius of 2.5 nm, such a surface charge density requires 57 ionized groups in the mouth); nonetheless, these calculations provide an indication of how effective charged groups might be in altering the electrical properties of the pore mouth and promoting ion access to the channel.

Possible Physiological Implications

The K^+ channel from SR and the Ca^{+2}-activated K^+ channel from TT exhibit high selectivity and high permeability (Coronado et al., 1980; Bell and Miller, 1984; Latorre et al., 1982; Vergara et al., 1984; Moczydlowski et al., 1985). The first property requires a narrow channel,

TABLE II
PEAK PORE MOUTH POTENTIAL, AS A FUNCTION OF PORE MOUTH GEOMETRY, FOR UNIFORM MOUTH SURFACE CHARGE DENSITY OF $2e/nm^2$

$b \equiv R/a_0$	Constriction entrance radius (nm)				
	0.15	0.2	0.25	0.3	0.4
	Potential (mV)				
2.5	201	268	335	402	536
5	431	574	718	861	1,149
7.5	669	892	1,115	1,338	1,784
10	911	1,214	1,518	1,821	2,429

whereas the second requires either a wide channel or a mechanism for concentrating ions near the constriction entrance. The constriction radius can be estimated from convergence conductance measurements (Läuger, 1976). The capture radius, the difference between the channel radius and the ionic radius, is

$$r_c = [\gamma/c]_0 \pi \lambda_0, \tag{10}$$

where $[\gamma/c]_0$ is the convergence conductance and λ_0, the limiting conductivity of the ion of interest. The ionic concentration, c, is the concentration near the constriction entrance, $c = c_B \exp(-eV/kT)$, where V is the electrical potential in this region. In terms of measurable quantities

$$r_c = [(\gamma/c_B)_0 \pi \lambda_0] \exp(eV/kT). \tag{11}$$

Thus, for cations, a negative potential in the mouth region increases the cation concentration near the constriction entrance; correspondingly, the capture radius could be reduced substantially.

The convergence conductances of the SR and TT K^+ channels suggest remarkably large capture radii, in the absence of an ion concentration mechanism. Table III lists estimated capture radii and channel radii for these systems assuming different values for the focussing potential near the mouth of the constriction. Blocking studies using quaternary ammonium probes (Miller, 1982*a*) suggested that the constriction radius in the SR channel is ~0.3 nm; there is presumably a narrower region within the constriction that acts as a selectivity filter. For the SR channel, a mouth potential of 10–15 mV increases K^+ concentration near the constriction 1.5-fold. The capture radius would then be ~0.15 nm; the constriction radius would be ~0.28 nm, consistent with the blocking studies. For the TT systems, a much larger mouth potential is needed to reduce the capture radius to a value consistent with the property of selectivity. If these channels are structurally similar to the SR systems, they may have a fairly wide entrance and a narrow selectivity neck well inside the constriction. However, even if the channel's radius is as large as 0.4 nm, as suggested by blocking studies (Vergara et al., 1984), a pore mouth potential of ~65 mV is required to increase K^+ concentration ~15-fold. For both SR and TT channels, capture and constriction radii deduced, assuming no mechanism for increasing ion concentration in the mouth, are large. For TT, the value is ridiculous, 3.7 nm! A pore with such dimensions would be an open shunt, not a highly discriminating channel.

TABLE III
CAPTURE AND CONSTRICTION RADII DETERMINED FROM CONVERGENCE CONDUCTANCE OF K^+ CHANNELS FROM SR AND TT AS FUNCTIONS OF PEAK PORE MOUTH POTENTIAL

Channel	Limiting conductivity	Peak pore mouth potential	Enrichment factor	Capture radius	Pore radius
	nS/M	*mV*		*nm*	*nm*
SR	5.5*	0	1	0.24	0.37
		−10	1.5	0.16	0.29
		−25	2.7	0.09	0.22
		−50	7.4	0.03	0.16
TT	83.2‡	0	1	3.60	3.73
		−50	7.4	0.49	0.62
		−65	13.5	0.27	0.40
		−75	20	0.18	0.31
		−100	55	0.07	0.20

*Bell and Miller, 1984.
‡Moczydlowski et al., 1985.

What kind of charge distributions can give rise to mouth potentials as large as 65 mV, the minimum needed to rationalize the TT data? If we imagine the electrical source to be focussed surface dipoles (Fig. 5 and Eq. 8b), we have already illustrated that with reasonable dipole densities and ideal dipolar alignment, which cannot be totally excluded (Wada, 1976; Hol, 1985), the resultant potential would be large enough, even if the interfacial dielectric constant is as large as 10; if dipole orientation is not ideal, this mechanism could not account for the observations at low K^+ concentration. If the electrical source is a fixed charge, the data of Table I indicate that any mouth geometry is adequate if the ionizable group is near the constriction entrance. If it is far from the pore mouth, the resultant pore mouth potential is too small unless the mouth itself is small (in which case the group cannot be too far from the entrance).

It is clear that any of the charge distributions considered can produce pore mouth potentials at least as large as 10–15 mV, needed to account for the observations on SR; there are no obvious grounds for distinction among the options. For TT, our general observations provide some grounds for discrimination. A focussed dipolar distribution might lower the pore mouth potential sufficiently; an ionizable group close to the entrance will do so; one far away will not.

Influence of Electrolyte Shielding

A negatively charged group or a suitable distribution of surface dipoles lowers the electrical potential near the entrance to the channel constriction. At low ionic strength, the influence of either source is great enough to rationalize the convergence conductance of either SR or TT channels. However, the dipolar mechanism is only marginally plausible for TT. Electrolyte shielding might substantially affect the pore mouth potential and greatly reduce the influence of the various sources. To determine the effect of Debye screening and to discriminate between dipolar sources and ionic sources, we have developed an approximate way of describing the effect that ionic strength has on pore mouth potentials. The method is outlined in the Appendix.

Most important is the substantial difference between electrolyte shielding of charges and of dipoles. As indicated in the Appendix for an entrance radius of 0.3 nm, changing

ionic strength from 10^{-2} to 1 M decreases the dipole potential 30–50%, depending upon mouth size; the corresponding figures for ionic sources are 75–90%. Sources that give rise to the same potential when $I = 0$ will be very different at accessible values of I. For the geometries studied, 100-fold changes in ionic strength affect dipole potentials about as much as 10-fold changes affect ionic potentials. Thus, the concentration dependence of the pore mouth potential can be different depending upon the nature of the electrical source. The ionic concentration at the constriction entrance is much less sensitive to ionic strength variation if the source is dipolar.

The cation concentration near the entrance to an SR channel can be increased if there is either a fixed charge or, near the pore entrance, a surface dipole layer. Conductance measurements using a variety of probes (Miller, 1982*a*,*b*) suggest an entrance radius of ~0.3 nm and a mouth size as large as 2 nm. From Table I, the peak pore mouth potential when $I = 0$ is ~73 mV for a charged group near the entrance (the value of b is 6.67). An ionic source far from the entrance gives rise to a ~20 mV potential when $I = 0$. The corresponding quantity for a dipolar source cannot be estimated without knowing the size of interfacial potential step (if any). Assuming the moderate value of 200 mV, the maximum mouth potential at $I = 0$ would be ~13 mV. All of these sources, as indicated in Table III, can adequately enhance cation concentration and rationalize convergence conductance data. Is there any way to discriminate among them? Fig. 8 presents Scatchard plots of γ/c_M vs. γ for the three possibilities using the data of Bell and Miller (1984); c_M is K^+ concentration at the constriction entrance calculated assuming that

$$c_M = c_K \exp[-e_0 V_A^*(I)/kT] \qquad (12)$$

where c_K is bulk K^+ concentration, $V_A^*(I)$ is the maximum (most negative) pore mouth potential, e_0 is the electronic charge, and kT is Boltzmann constant times temperature. The local concentration, c_M, determines channel conductance. As long as the channel operates by a single ion mechanism, simple Michaelis-Menton kinetics should apply (Coronado et al., 1980). If this is so, Scatchard plots are linear; the intercept is the convergence conductance. If the fixed charge is near the channel entrance, the plot is highly nonlinear; this hypothesis can be excluded as a device for attracting cations to the channel mouth. Either a dipolar source near the entrance or a fixed charge, in the mouth, but far from the entrance, is plausible. Both Scatchard plots are linear; the convergence conductances imply entrance radii of ~0.3 nm in each instance.

Is there any way to distinguish between these alternatives? Multi-valent cations might affect channel conductance somewhat differently. If there were a fixed negative charge in the mouth fairly far from entrance, an M^{+n} ion could bind there and reverse the polarity of the pore mouth potential. If there were simply a dipolar distribution near the entrance, multivalent ions would have no specific effect

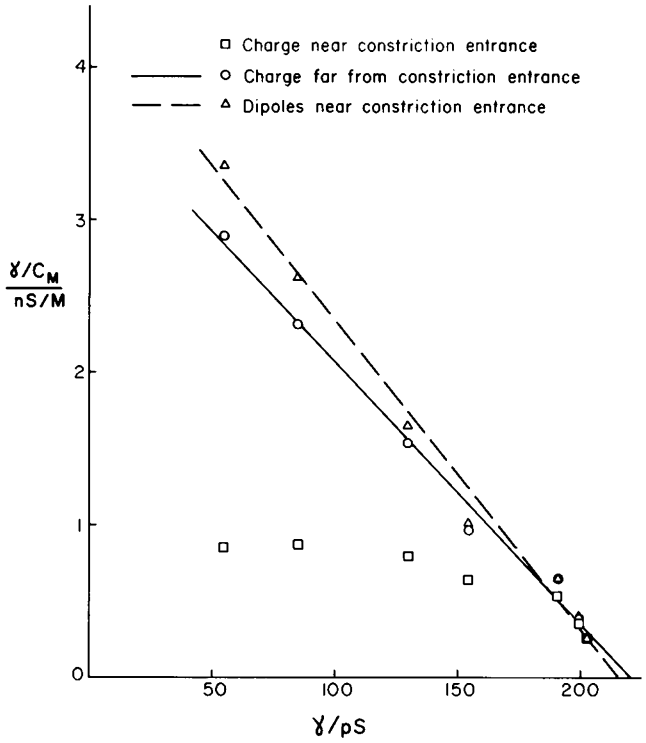

FIGURE 8 Scatchard plot of γ/c_M vs. γ for the K^+ channel of SR; c_M is the maximum pore mouth concentration of K^+ (see text). Three hypotheses are contrasted. The data are those of Bell and Miller (1984). The straight lines represent least squares fits.

other than their influence on ionic strength. Thus, multivalent ions should lower channel conductance in the first case; they should have little effect in the second. Unfortunately, simple cations appear to enter and block the channel rather than bind in the mouth (Coronado et al., 1980). However, experiments with bis-primary amino alkyl ions suggest that these divalent species do not block the channel at a deep site.[3] Instead they appear to reduce single channel conductance in a voltage-independent manner, indicative of the presence of a fixed charge in the further regions of the channel mouth. Further study of this phenomenon might provide definitive evidence for the presence of a fixed negative charge in the mouth.

While our treatment is based upon charge distributions, not point charges, it is still possible to estimate the location of the postulated fixed charge. Given the parameters used to describe the SR channel mouth, the center of charge is the widest part of the vestibule, a z-distance of ~1.9 nm from the constriction entrance. The total distance from the entrance would be ~2.5 nm. At zero ionic strength, and without nearby lipid to repel lines of force, the electrical potential due to a charge at this location would be only ~7 mV at the center of the entrance. The maximum axial potential it could create in the pore mouth would be ~11 mV.

[3]Miller, C., personal communication.

Can more be said about how the TT channel develops such large conductances? As indicated, only the presence of a fixed negative charge close to the channel entrance is likely to create a pore mouth potential large enough to rationalize the convergence conductance (although a dipolar mechanism cannot be immediately ruled out). As the channel is blocked by various TEA derivatives (Vergara et al., 1984), an entrance radius between 0.3 and 0.4 nm is not unreasonable. Studies that contrast the properties of the channel when it is inserted into neutral and negatively charged membranes suggest a mouth size of ~1 nm (Moczydlowski et al., 1985). Scatchard plots of γ/c for rat TT reconstituted in phosphatidylethanolamine (PE) membranes are not linear (Moczydlowski et al., 1985), indicative of complex channel kinetics. If deviations from Michaelis–Menton kinetics were only due to shielding of a mouth charge (or of surface dipoles), Scatchard plots of γ/c_M should be linear. We have tested these ideas using the data of Moczydlowski et al. (1985),[4] assuming either a fixed negative charge near the channel entrance or a focussed dipolar layer; the geometric parameters are an a_0 of 0.4 nm and a mouth size of 1 nm. In both cases, the plots, even taking shielding into consideration, are far from linear.

However, a negatively charged group in the pore mouth provides another mechanistic basis for the observed kinetics, one that is not reasonable if the electrical source is a layer of surface dipoles. What if the charged group is also a binding site for K^+? If such a binding site existed, the channel might exist in two conducting states that equilibrate too rapidly to be separately observable, negatively charged (T_-) and neutral (T_0),

$$T_0 = T_- + K^+, \text{ equilibrium constant, } K.$$

For the neutral channel, there is no focussing field; K^+ concentration in the vestibule and in the bulk solution are equal. For the negatively charged channel, K^+ concentration in the vestibule is greater than that in the bulk solution. If both neutral and negatively charged forms are single ion channels, the conductance is

$$\gamma = \sigma_\infty\{[1/(1 + K_-/C_M)] + (C/K)[1/(1 + K_0/C)]\}\,[1/(1 + C/K)], \quad (13)$$

where C_M is given by Eq. 12 and C is the bulk K^+ concentration. We assume that both open states have the same limiting conductance, but that they may have different affinities for K^+; alternatively, K_- and K_0 may be assumed to be the same. Fig. 9 presents the data in two ways, a conductance–concentration plot and a Scatchard plot; a_0 is 0.4 nm and the mouth size is 1 nm. The fit is just as good for the three parameter form ($K_- \equiv K_0$); changing a_0 has no significant effect. The model parameters for two

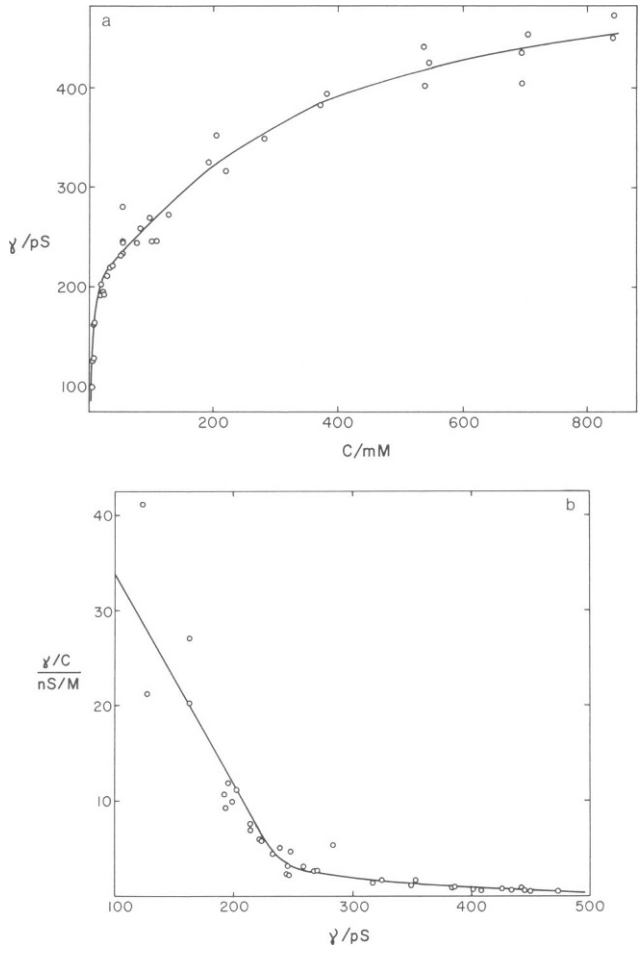

FIGURE 9 (*a*) Conductance-concentration and (*b*) Scatchard plots for the Ca^{+2}-activated K^+ channel from TT assuming that the channel exists in two rapidly equilibrating conducting forms (see text). The mouth parameters are a_0 = 0.4 nm and R = 1 nm. The charge distribution is concentrated near the entrance to the constriction. The curve is the least squares fit of the data to Eq. 13.

values of a_0 are listed in Table IV; both cases, K_0 and K_- dependently and independently variable, are considered. Lower bounds on the channel radius are estimated from Eqs. 9 and 10. All model properties are consistent with the data. Given the uncertainty in the parameters, the three and four parameter forms are essentially indistinguishable. Since the vestibule binding site has a binding constant of

TABLE IV
PARAMETERS DETERMINED BY NONLINEAR LEAST SQUARES FITS OF EQ. 13 TO CONDUCTANCE DATA FOR CA^{+2}-ACTIVATED K^+ CHANNEL FROM TT*

a_0/nm	K/mM	σ_∞/pS	K_-/mM	K_0/mM	r/nm
0.3	58	539	219	157	>0.28
	54	578	214‡	214‡	>0.24
0.4	47	539	107	161	>0.34
	52	505	115‡	115‡	>0.32

*Two rapidly equilibrating conducting states are assumed
‡In this parameterization, $K_- \equiv K_0$.

[4]I want to thank Dr. E. Moczydlowski for making his original data available to me.

~50 mM, binding of Ca^{+2} is unlikely as it is only in micromolar concentrations.

The center of charge again provides a way to roughly estimate the position of the postulated fixed charge. For the TT geometries analyzed, this point is located a z-distance of ~0.9 nm from the constriction entrance. The linear distance from the center of the entrance is ~1.05 nm. Even at zero ionic strength, in the absence of the surrounding lipid, such a charge would create an axial pore mouth potential at the entrance of only ~17 mV; the maximum axial potential in the pore mouth would be only ~30 mV. Only because lines of force are repelled from the low ϵ domain can the pore mouth potentials attain the values needed to act as powerful ion attractors.

SUMMARY

We have analyzed the effect that various electrical sources may have on ion permeation up to and through transmembrane channels.

(*a*) We have extended our treatment of the water–lipid potential difference (membrane dipole potential) to account for vestibule influence. The theory adequately explains the effect of membrane dipole potential variation of both gramicidin-B (Bamberg et al., 1976) and gramicidin-M^- (see footnote 2) channels.

(*b*) We have shown that the low dielectric lipid domain amplifies the electrical potential due to surface charges or surface dipoles located in the pore mouth. The potential is two to four times as large as it would be were the source surrounded only by water.

(*c*) A surface dipole distribution concentrated near the constriction entrance or a fixed charge far from the constriction entrance can raise $[K^+]$ sufficiently to account for the large convergence conductance of the K^+ channel from sarcoplasmic reticulum. Consideration of electrolyte shielding does not affect this conclusion. Conductance measurements in the presence of certain divalent cations might permit discrimination of the two hypotheses.

(*d*) A fixed charge located near the constriction entrance raises $[K^+]$ enough to account for the convergence conductance of the Ca^{+2}-activated K^+ channel from transverse tubule. Again, considerations of electrolyte shielding do not alter this conclusion. We suggest that the fixed charge in the vestibule can bind K^+; this hypothesis permits us to account for observed deviations from simple Michaelis-Menton kinetics.

APPENDIX

Electrolyte Shielding

Consider a system with geometry illustrated in Fig. 10 *a*, a planar annulus with an arbitrary cylindrically symmetric charge (or dipole) distribution located between a_0 and $R_0 = a_0 + R$. The right-hand region is aqueous electrolyte of ionic strength I; the left-hand region is lipid. This model has the virtue of being exactly soluble for arbitrary charge distributions. While obviously not the same as the mouth geometries considered in this paper, some approximate correspondences can be made as shown in Fig. 10 *b*.

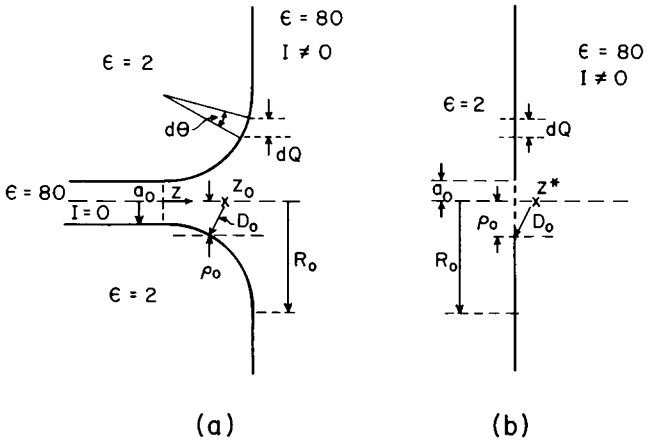

FIGURE 10 Geometries for (*a*) original and (*b*) substituted systems for estimating effects of electrolyte shielding. The electrical source is distributed on the surfaces between a_0 and R_0 in both cases. The differential source element dQ is the same in both cases, necessitating a greater source concentration in the substitute geometry. An axial point z_0 in the original geometry is closest to a point in the flared mouth at ρ_0; the distance is D_0. The equivalent point in the substitute system is z^*, a distance D_0 from the ring at ρ_0. In the original system, $\epsilon = 80$ in the cylinder of radius $\rho \leq a_0$ for which $z < 0$. In the substitute system, this region has an $\epsilon = 2$.

The differential element of charge in Fig. 10 *b* is

$$dQ = \sigma_0 f(\theta) b d\phi \rho d\theta = \sigma_0 f(\theta) d\phi \sec\theta \, \rho d\rho \quad \text{(A1a)}$$

$$w(\rho) = \sec\theta = \{1 - [(R_0 - \rho)/R]^2\}^{-1/2}. \quad \text{(A1b)}$$

Because the derivative of arc length with respect to ρ is larger as $\rho \to a_0$, the radial concentration of charge is greater for smaller values of ρ. A uniform charge distribution in the original system is replaced by a nonuniform one in the substitute system; the factor is $w(\rho)$.

A correspondence between axial distance in the two systems is also needed. A point z_0 from constriction entrance in Fig. 10 *b* is clearly much closer to the electrical source than a point the same distance away from the planar annulus in Fig. 10 *a*. The distinction is obviously due to the fact that, in the geometries of physical interest, the pore mouth flairs outward. At a point z_0 in Fig. 10 *b*, the distance of closest approach to the mouth is $D_0 = \sqrt{R_0^2 + z_0^2} - R$; the corresponding value of ρ is $\rho_0 = R_0 D_0 \sqrt{R_0^2 + z_0^2}$. We assume approximately equivalent shielding takes place at a point z in the planar system a distance D_0 from the ring $\rho = \rho_0$ on the planar surface; the result is

$$z = z_0 [1 - R/\sqrt{R_0^2 + z_0^2}]. \quad \text{(A2)}$$

When $z_0 >> R_0$, there is no difference between z and z_0; the z/z_0 ratio is smallest for $z_0 = 0$.

Finally, there is another difference between the geometries of Fig. 10, *a* and *b*. In Fig. 10 *b*, there are two electrical phases to the left of the constriction entrance: the pore water for which $\epsilon = 80$ and the lipid for which $\epsilon = 2$. In the substitute system, there is only lipid. The polarization charges at the dielectric discontinuity must affect the electrical potential in the aqueous phase. If we imagine that they can be treated as if they altered the surface charge distribution at the pore mouth–water interface and that electrolyte shielding could then be accounted for by considering only the electrolyte itself, the axial potential would be

$$\psi(I; z_0) = \psi(I = 0; z_0) F(I, z_0), \quad \text{(A3)}$$

where $F(I,z_0)$ is a shielding factor determined by the charge distribution, the electrolyte composition and the geometry. Using Eqs. A1 and A2 to effect the correspondence between curved and planar geometries, the shielding factor can be estimated from the properties of the annular system. The charge distribution is given by Eq. A1 and the effective value of z by Eq. A2.

The calculation of the shielding factor in the substitute system is straightforward. The Poisson-Boltzmann equation describes the electrical potential in an aqueous electrolyte (McLaughlin, 1977). As long as the ionic strength is not too high, the equation can be linearized with the result

$$\nabla^2\psi = \kappa^2\psi, \qquad \kappa^2 = 2 \times 10^3 F^2 I/\epsilon_0\epsilon_1 RT. \tag{A4}$$

κ^{-1} is the Debye length and concentrations are measured in molarity. For the geometry of Fig. 10 *a*, the general solution, since the potential is finite for $\rho = 0$, $\rho = \infty$, and $z = \infty$, is

$$\psi(\rho,z) = Ae^{-\kappa z} + \int_0^\infty d\mu B(\mu) J_0(\rho\mu) e^{-z\lambda(\mu)}, \tag{A5}$$

where $\lambda = \sqrt{\kappa^2 + \mu^2}$ and J_0 is the Bessel's function of order zero (Abramowitz and Stegun, 1965). For nonuniform surface charges located on the annulus,

$$\sigma = \sigma_0 f(\rho) w(\rho), \qquad a_0 \le \rho \le R_0 \tag{A6a}$$

$$\sigma = 0, \qquad \rho < a_0, \qquad \rho > R_0, \tag{A6b}$$

the coefficients A and $B(\mu)$ are established by the electric field at the surface, $z = 0$,

$$\delta\psi/\delta z|_{z=0} = -(\sigma_0/\epsilon_0\epsilon_1) f(\rho) w(\rho), \tag{A7}$$

which with Eq. 5 yields

$$\kappa A + \int_0^\infty d\mu B(\mu)\lambda(\mu) J_0(\rho\mu) = (\sigma_0/\epsilon_0\epsilon_1) g(\rho) w(\rho)$$

$$a_0 \le \rho \le R_0 \tag{A8a}$$

$$\kappa A + \int_0^\infty d\mu B(\mu)\lambda(\mu) J_0(\rho\mu) = 0 \qquad \rho \le a_0, \quad \rho > R_0 \tag{A8b}$$

In this formulation, $w(\rho)$ accounts for the fact that, in the original geometry, charge is more concentrated at small ρ values; $f(\rho)$ describes whatever non-uniformity was present in the original system. As $J_0(\rho\mu) \to 0$ for $\rho \to \infty$, $A = 0$; using the δ-function property of the Bessel's function (Erdelyi et al., 1954), the solution to Eq. 4 is

$$\lambda(\mu)B(\mu)/\mu = (\sigma_0/\epsilon_0\epsilon_1) \int_{a_0}^{R_0} d\rho\rho g(\rho) w(\rho) J_0(\rho\mu). \tag{A9}$$

The shielded electrical potential due to surface charges in the ring is thus

$$\psi_c(r,z) = (\sigma_0/\epsilon_0\epsilon_1) \int_{a_0}^{R_0} d\rho\rho g(\rho) w(\rho) \cdot \int_0^\infty d\mu \{\mu e^{-z\lambda(\mu)}/\lambda(\mu)\} J_0(r\mu) J_0(\rho\mu). \tag{A10}$$

As long as consideration is limited to the axis, the μ-integration can be carried out (Erdelyi et al., 1954) with the result

$$\psi_c(0,z) = (\sigma_0/\epsilon_0\epsilon_1) \int_{a_0}^{R_0} d\rho\rho g(\rho) w(\rho) (1/\sqrt{z^2 + \rho^2}) e^{-\kappa\sqrt{z^2+\rho^2}}. \tag{A11}$$

The potential due to a distribution of surface dipoles can be calculated from Eqs. A10 or A11 by placing rings of positive and negative charge at $z = \pm\delta$; thus,

$$\psi_D(r,z) = \lim_{\delta\to 0} [\psi_c(r, z+\delta) - \psi_c(r, z-\delta)] \tag{A12}$$

and using Eq. A11, the axial potential is

$$\psi_D(0,z) = (\mu_0 z/\epsilon_0\epsilon_1) \int_{a_0}^{R_0} d\rho\rho g(\rho) w(\rho) [e^{-\kappa\sqrt{z^2+\rho^2}}/(z^2+\rho^2)](\kappa + 1/\sqrt{z^2+\rho^2}). \tag{A13}$$

Electrolyte shielding is substantially different depending upon whether the electrical source is a set of charges or dipoles. This can be most clearly seen in the simplest instance, $g(\rho)w(\rho) = 1$. In this case

$$\psi_c(0,z) = (\sigma_0/\epsilon_0\epsilon_1)(e^{-\kappa R_A} - e^{-\kappa R_B})/\kappa \tag{A14a}$$

$$R_A = \sqrt{z^2 + a_0^2}, \qquad R_B = \sqrt{z^2 + R_0^2} \tag{A14b}$$

$$\psi_D(0,z) = (\mu_0 z/\epsilon_0\epsilon_1)(e^{-\kappa R_A}/R_A - e^{-\kappa R_B}/r_B). \tag{A15}$$

As long as R_0 is large enough that the second term in each of these expressions can be ignored, quantitative comparisons of the effect of ionic strength variation are easily made. The major distinction is that, for surface charges, the potential is proportional to the Debye length, κ^{-1}; for surface dipoles it is not. Table V compares the effect of shielding for a_0 representative of entrance radii for the channels of interest. The numbers tabulated are relative shielding factors, $F^*(I) \equiv \psi^*(I)/\psi^*(10^{-3}\text{ M})$; the ψ's contrasted are the maximum values of the respective pore mouth potentials. Differences are dramatic. Depending upon the value of a_0, 10-fold concentration changes more significantly attenuate the ionic potential than 1,000-fold changes attenuate the dipolar potential. The shielded ionic potential decreases 12- to 15-fold as ionic strength increases from 1 to 100 mM; over the same concentration range, the shielded dipole potential decreases by less than a factor of 2.

TABLE V

RELATIVE SHIELDING FACTORS FOR IONIC AND DIPOLAR POTENTIALS AS A FUNCTION OF IONIC STRENGTH AND CONSTRICTION ENTRANCE RADIUS*

I/mM	Ionic source			Dipolar source		
	Constriction entrance radius, a_0 (nm)					
	0.2	0.3	0.4	0.2	0.3	0.4
1	≡ 1	≡ 1	≡ 1	≡ 1	≡ 1	≡ 1
10	0.30	0.30	0.29	0.87	0.84	0.80
100	0.083	0.076	0.069	0.64	0.55	0.48
1,000	0.017	0.012	0.009	0.31	0.20	0.14

*Shielding is measured with respect to systems at 1 mM ionic strength.

We wish to thank C. Miller, O. S. Andersen and E. Moczydlowski for helpful comments; I especially appreciate the latter's suggestions with respect to vestibule effects in the TT system.

This work has been supported by the National Institutes of Health, GM-28643.

Received for publication 3 February 1986 and in final form 17 September 1986.

REFERENCES

Abramowitz, M., and I. A. Stegun. 1965. Handbook of Mathematical Functions. Dover Publications, Inc., New York. 1046 pp.

Andersen, O. S., A. Finkelstein, I. Katz, and A. Cass. 1976. Effect of phloretin on the permeability of thin lipid membranes. *J. Gen. Physiol.* 67:749–771.

Andersen, O. S. 1978. Ion transport across simple membranes. *In* Renal Function. G. H. Giebisch and E. F. Purcell, editors. Josiah Macy Foundation, New York. 71–99.

Andersen, O. S. 1983. Ion movement through gramicidin A channels. Studies on the diffusion controlled association step. *Biophys. J.* 41:147–165.

Amstrong, C. M. 1975. Ionic pores, gates and gating currents. *Quart. Rev. Biophys.* 7:179–210.

Bamberg, E., K. Noda, E. Gross, and P. Lauger. 1976. Single channel parameters of gramicidin A, B and C. *Biochim. Biophys. Acta.* 418:223–228.

Bell, J. E., and C. Miller. 1984. Effects of phospholipid surface charge on ion conduction in the K^+ channel of sarcoplasmic reticulum. *Biophys. J.* 45:279–287.

Benz, R., O. Frohlich, P. Läuger, and M. Montal. 1975. Electrical capacity of black lipid films and of lipid bilayers made from monolayers. *Biochim. Biophys. Acta.* 394:323–334.

Coronado, R., R. L. Rosenberg, and C. Miller. 1980. Ionic selectivity, saturation and block in a K^+ channel from sarcoplasmic reticulum. *J. Gen. Physiol.* 76:425–446.

Erdelyi, A., W. Magnus, F. Oberhettinger, and F. G. Tricomi. 1954. Table of Integral Transforms. Vol. 2. McGraw-Hill Book Co., New York. 5–9.

Flewelling, R. F., and W. L. Hubbell. 1986. The membrane dipole potential in a total membrane potential model. Applications to hydrophobic ion interactions with membranes. *Biophys. J.* 49:541–552.

Heitz, F., F. Spach, and Y. Trudelle. 1982. Single channels of 9,11,13,15-destryptophyl-phenalanyl gramicidin A. *Biophys. J.* 40:87–89.

Heitz, F., F. Spach, and Y. Trudelle. 1984. Single channels of various gramicidins. Voltage effects. *Biophys. J.* 45:97–99.

Hille, B., and E. Schwartz. 1978. Potassium channels as multi-ion single-file pores. *J. Gen. Physiol.* 72:409–442.

Hol, W. G. J. 1985. The role of the α-helix dipole in protein function and structure. *Prog. Biophys.* 45:149–195.

Jordan, P. C. 1982. Electrostatic modeling of ion pores. Energy barriers and electric field profiles. *Biophys. J.* 39:157–164.

Jordan, P. C. 1983. Electrostatic modeling of ion pores. II. Effects attributable to the membrane dipole-potential. *Biophys. J.* 41:189–195.

Jordan, P. C. 1984*a*. The total electrostatic potential in a gramicidin channel. *J. Membr. Biol.* 78:91–102.

Jordan, P. C. 1984 *b*. The effect of pore structure on energy barriers and applied voltage profiles. I. Symmetrical channels. *Biophys. J.* 45:1091–1100.

Jordan, P. C. 1985. Why is a channel both highly selective and highly permeable? The effect of pore mouth charge distribution. *Biophys. J.* 47(2, Pt. 2):385*a*. (Abstr.)

Jordan, P. C. 1986. Ion channel electrostatics and the shape of channel proteins. *In* Ion Channel Reconstitution. C. Miller, editor. Plenum Publishing Corp., New York. 37–55.

Kistler, J., and R. M. Stroud. 1981. Crystalline arrays of membrane-bound acetylcholine receptor. *Proc. Natl. Acad. Sci. USA.* 78:3678–3682.

Koeppe, R. C., K. O. Hodgson, and L. Stryer. 1978. Helical channels in crystals of gramicidin A and of a cesium-gramicidin A complex: an x-ray diffraction study. *J. Mol. Biol.* 121:41–54.

Latorre, R., C. Vergara, and C. Hildalgo. 1982. Reconstitution in planar lipid bilayers of a Ca^{+2}-dependent K^+ channel from transverse tubule membranes isolated from rabbit skeletal muscle. *Proc. Natl. Acad. Sci. USA.* 79:805–809.

Läuger, P. 1976. Diffusion-limited ion flow through pores. *Biochim. Biophys. Acta.* 455:493–509.

Lee, W. K., and P. C. Jordan. 1984. Molecular dynamics simulation of cation motion in water-filled, gramicidin like pores. *Biophys. J.* 46:805–819.

Levitt, D. G. 1978. Electrostatic calculations for an ion channel. I. Energy and potential profiles and interaction between ions. *Biophys. J.* 22:209–219.

Levitt, D. G. 1985. Strong electrolyte continuum theory solution for equilibrium profiles, diffusion limitation and conductance in charged ionic channels. *Biophys. J.* 48:19–31.

MacKay, D. H. J., P. Berens, K. R. Wilson, and A. T. Hagler. 1984. Structure and dynamics of ion transport through gramicidin A. *Biophys. J.* 46:229–248.

McLaughlin, S. A. 1977. Electrostatic potentials of membrane-solution interfaces. *Curr. Top. Membr. Transp.* 9:71–144.

Miller, C. 1982*a*. Bis-quaternary ammonium blockers as structural probes of the sarcoplasmic reticulum K^+ channel. *J. Gen. Physiol.* 79:869–891.

Miller, C. 1982*b*. Feeling around inside a channel in the dark. *In* Transport in Biological Membranes. R. Antolini, editor. Raven Press, New York. 99–108.

Moczydlowski, E., O. Alvaraz, C. Vergara, and R. Latorre. 1985. Effect of phospholipid surface charge on the conduction and gating of a Ca^{+2} activated K^+ channel in planar lipid bilayers. *J. Membr. Biol.* 83:273–282.

Parsegian, V. A. 1969. Energy of an ion crossing a low dielectric membrane: solution to four relevant electrostatic problems. *Nature (Lond.).* 221:844–846.

Pethig, R. 1979. Dielectric and Electronic Properties of Biological Materials. John Wiley & Sons, Chichester, England. 44–49.

Pickar, A. D., and R. Benz. 1978. Transport of oppositely charged lipophilic ion probes in lipid bilayers having various structures. *J. Membr. Biol.* 44:353–376.

Tredgold, R. H., and P. V. Hole. 1976. Dielectric behavior of dry synthetic polypeptides. *Biochim. Biophys. Acta.* 443:137–142.

Urry, D. W. 1971. The gramicidin A transmembrane channel: a proposed $\pi_{(L,D)}$, helix. *Proc. Natl. Acad. Sci. USA.* 68:672–676.

Urry, D. W., S. Alonso-Romanowski, C. W. Venkatachalam, T. L. Trapane, R. D. Harris, and K. U. Prasad. 1984. Shortened analog of the gramicidin A channel argues for the doubly occupied channel as the dominant conducting state. *Biochim. Biophys. Acta.* 775:115–119.

Vergara, C., E. Moczydlowski, and R. Latorre. 1984. Conduction, blockade and gating in a Ca^{+2}-activated K^+ channel incorporated into planar lipid bilayers. *Biophys. J.* 45:73–76.

Wada, A. 1976. The α-helix as an electric macrodipole. *Adv. Biophys.* 9:1–63.

Wada, A., and H. Nakamura. 1981. The nature of the charge distribution in proteins. *Nature (Lond.).* 293:757–758.

Wallace, B. A. 1976. The structure of gramicidin A. *Biophys. J.* 49:295–306.